Published online October 19, 2004

5658–5667 *Nucleic Acids Research, 2004, Vol. 32, No. 18*
doi:10.1093/nar/gkh898

Concerted bis-alkylating reactivity of clerocidin towards unpaired cytosine residues in DNA

Sara N. Richter, Ileana Menegazzo[1], Daniele Fabris[2] and Manlio Palumbo*

Department of Pharmaceutical Sciences and [1]Department of Chemical Sciences, University of Padova, 35131 Padova, Italy and [2]Department of Chemistry and Biochemistry, University of Maryland, Baltimore County, Baltimore, MD 21250, USA

Received July 8, 2004; Revised and Accepted September 30, 2004

ABSTRACT

Clerocidin (CL) is a topoisomerase II poison, which cleaves DNA irreversibly at guanines (G) and reversibly at cytosines (C). Furthermore, the drug can induce enzyme-independent strand breaks at the G and C level. It has been previously shown that G-damage is induced by alkylation of the guanine N7, followed by spontaneous depurination and nucleic acid cleavage, whereas scission at C is obtained only after treatment with hot alkali, and no information is available to explain the nature of this damage. We present here a systematic study on the reactivity of CL towards C both in the DNA environment and in solution. Selected synthetic derivatives were employed to evaluate the role of each chemical group of the drug. The structure of CL–dC adduct was then characterized by tandem mass spectrometry and NMR: the adduct is a stable condensed ring system resulting from a concerted electrophilic attack of the adjacent carbonyl and epoxide groups of CL towards the exposed NH_2 and N3, respectively. This reaction mechanism, shown here for the first time, is characterized by faster kinetic rates than alkylation at G, due to the fact that the rate-determining step, alkylation at the epoxide, is an intramolecular process, provided a Schiff base linking CL and C can rapidly form, whereas the corresponding reaction of G N7 is intermolecular. These results provide helpful hints to explain the reversible/irreversible nature of topoisomerase II mediated DNA damage produced by CL at C/G steps.

INTRODUCTION

Clerocidin (CL) is a microbial terpenoid with potent antibacterial and antitumor activity (1). Previous investigations have shown that this chemical is capable of poisoning both the prokaryotic DNA gyrase and the eukaryotic DNA topoisomerase II (2–4). As a result, CL induces enzyme-mediated DNA damage with a distinct cleavage pattern (4), which is unique within the class of topoisomerase II inhibitors. Unlike with other inhibitors, CL-stimulated cleavage appears to be less sensitive to ionic strength, as shown by the fact that only selected sites revert upon salt addition, while activity toward most sites remains largely unaffected. In particular, it was observed that the base immediately preceding the site of enzymatic attack (i.e. position −1) was always a guanine (G) in the case of irreversible cleavage sites, whereas a cytosine (C) was normally found at reversible, salt-sensitive sites (5), thus suggesting two distinct mechanisms for CL-stimulated damage. Further support to this hypothesis is provided by the fact that, while CL alkylation of guanine N7 induces direct depurination and leads to strand scission at the apurinic site in the absence of the enzyme, similar enzyme-independent cleavage of C-alkylated substrates requires treatment with hot alkali (6). Understanding the chemical reasons for such an exceptional biological behavior would be particularly important to evaluate the possibility of modulating CL activity.

The structure of CL (Figure 1A) displays several electrophilic groups, which include an α-ketoaldehyde function in equilibrium with the hemi-acetalic form, a strained epoxy ring (region C12–C15) and a second aldehyde at position 4 of the diterpenoid structure. It was recently shown that the oxirane is solely responsible for the guanine alkylating activity, whereas the vicinal carbonyl functions are crucial in modulating the rates of reactivity by finely tuning the strain applied to the epoxide ring (7). The aldehyde of the diterpenoid structure is not necessary for drug activity, since natural congeners devoid of this functional group (i.e. terpentecin and UCT4B) are still capable of poisoning topoisomerase II (2,4,8). Moreover, a synthetic CL-analogue in which a naphthalene ring replaced the diterpenoid moiety was able to alkylate DNA *per se* (7).

Earlier work was mainly focused on studying the prominent reaction of CL with guanine, leading to propose a mechanism for the irreversible cleavage stimulation at this nucleotide (6,7). No concerted effort was made to explain the salt-sensitive nature of the strand scission at cytidine. We are now presenting a systematic study of the reactivity of CL towards C, which employs selected synthetic derivatives to assess the role of each chemical group. In particular, the C12–C15 ring of CL was modified to include either an intact (NA1, NA2 and NA3, Figure 1B), or an open epoxide ring (NA4 and NA5, Figure 1C). The oxidation state of the carbonyls was varied in each series from fully oxidized (CL-like, such as NA1 and NA4), to partially (NA2 and NA5) and fully reduced (NA3). CL and its synthetic derivatives were tested for their ability to react with cytosine in single- and

*To whom correspondence should be addressed. Tel: +39049 827 5711/7; Fax: +39049 827 5366; Email: manlio.palumbo@unipd.it

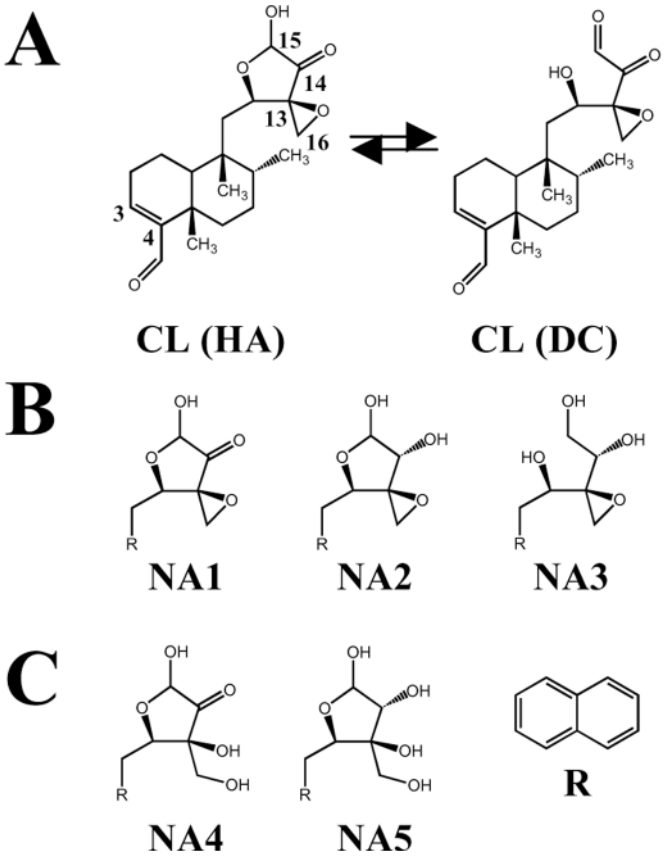

Figure 1. Structures of CL and NA derivatives. (**A**) The dicarbonylic form of the drug (DC) is shown in equilibrium with the closed hemi-acetal species (HA). Numbered positions outline electrophilic carbons. (**B**) Intact epoxide naphthalene derivatives. (**C**) Open epoxide naphthalene derivatives. The carbonyl functions are unmodified in NA1 and NA4, partially reduced in NA2 and NA5, and fully reduced in NA3.

double-stranded oligonucleotides and to induce strand cleavage with and without alkali treatment. The structure of adducts formed with C nucleosides in solution was characterized by tandem mass spectrometry and NMR to gain valuable insights on the structural determinants of CL reactivity toward C and help to explain its mechanism of action at this nucleotide.

MATERIALS AND METHODS

Chemicals, oligonucleotides and enzymes

CL was a gift of Leo Pharmaceutical Products (Ballerup, Denmark). NA (naphthalene) analogues were generously provided by Prof. S. Kobayashi (University of Tokyo, Japan). CL and NA analogues were dissolved in absolute ethanol and the concentration determined by measuring absorbance in ethanol at 230 and 282 nm on a UV/VIS Spectrometer Lambda 12 (Perkin Elmer, MA, USA). Molar extinction coefficients were experimentally determined to be 11 818 M^{-1} cm^{-1} for CL and 9493 M^{-1} cm^{-1} for NA derivatives. Working drug solutions were obtained by diluting fresh stocks in the appropriate buffer. Buffer components, nucleosides, chemicals for MS calibration and NMR analysis were purchased from Sigma-Aldrich (St Louis, MO, USA), while electrophoretic reagents were from Amersham Biosciences Europe (Freiburg, Germany). T4 polynucleotide kinase was purchased from Invitrogen (Paisley, UK). [γ-^{32}P]ATP was from Perkin Elmer (MA, USA), while all oligonucleotides were from Eurogentec (Liege, Belgium). HPLC purity solvents were from LabScan (Dublin, Ireland). ^{15}N-dC was purchased from Chemical Research (Spectra Stable Isotopes, MD, USA).

Sequencing reactions with oligonucleotides

The ability of CL and NA derivatives to damage DNA at the C-level was tested using short oligonucleotide substrates, whose sequences span a strong irreversible site for CL cleavage in the presence of murine topo II (position 2640 in the SV40 genome) (5). The following oligonucleotides: CTA TTG CTT TAT TTG TAA CCA TTA TAA GCT (CL2640-up), CTA TTG CTT TAT TTC TAA CCA TTA TAA GCT (CL2640-up-C), and AGC TTA TAA TGG TTA ATA AAG CAA TAG (CL2640-B-down) were appropriately annealed to form a stable duplex with either a TGT bulge (CL-2640-up and CL2640-B-down), or a TCT bulge (CL-2640-up-C and CL2640-B-down; in each case the three extruded nucleotides are underlined).

All oligonucleotides were gel-purified before use and prepared in desalted/lyophilized form. CL2640-up and CL2640-up-C were 5′ end-labeled with [γ-^{32}P]ATP by T4 polynucleotide kinase and were subsequently purified by ethanol precipitation. Either bulged-duplex substrate was obtained by annealing the labeled CL2640-up or CL2640-up-C oligonucleotides with equimolar amounts of their complementary cold oligonucleotide (CL2640-B-down). The annealed species were further purified in native polyacrylamide gels and electro-eluted using the Biotrap method (Schleicher & Schuell, NH, USA).

Drug reactions with the labeled single-stranded (CL2640-up) or bulged substrates (4 pmol/sample) were performed at 37°C in 50 mM phosphate buffer, pH 7.4, containing 80 mM KCl and 10 mM $MgCl_2$. These conditions were selected to maintain the stability of the target oligonucleotide structures and to minimize the possible competition of buffer molecules for drug alkylation (9). At the indicated time intervals, samples were ethanol precipitated to eliminate non-reacted drug, then resuspended and either kept on ice, or treated at 90°C for 30 min with 1 M piperidine to complete strand scission according to the Maxam and Gilbert protocol (10). Samples were then lyophilized twice, resuspended in formamide gel-loading buffer, and heated at 90°C for 5 min. The reaction products were analyzed on 20% denaturing polyacrylamide gels and visualized by phosphorimaging analysis (Molecular Dynamics, Amersham Biosciences, Europe). Quantification was performed by ImageQuant software (Molecular Dynamics). For piperidine kinetics analysis, 1 M piperidine treatment was performed at 90°C for 0.4, 0.2, 1, 2, 3 h.

HPLC, LC–MS, ESI–MS and tandem mass spectrometry

CL and the NA series derivatives were dissolved in 50 µl ethanol and diluted with a 11 mM solution of dC in 50 mM HEPES (pH = 7.4) to provide a final drug concentration of 0.1 mM and a 1:100 drug to substrate molar ratio. Each mixture was incubated at 37°C, while aliquots were taken at

increasing incubation intervals. These sample mixtures were filtrated on 0.45 μm filters (Alltech, Dunboyne, Ireland) and loaded on a HPLC C18 reverse phase column (Extent-C18, 4.6 × 250 mm, Agilent Technologies, CA, USA). The HPLC system included a Series 200 Pumps (Perkin Elmer, CA, USA); UV-1806, UV-Vis Detector (Bio-Rad, Milan, Italy) and a NCI 900 Network Chromatography Interface (Perkin Elmer, CA, USA). A mobile phase composed by different percentages of A [CH_3CN:H_2O (9:1)/0.05% TFA] and B [H_2O/0.05% TFA] and delivered at a flow rate of 1 ml/min was used to achieve the separation of the different reaction products. In particular, the following gradients were used for the analysis of CL and NA1 solutions: A 20% for 8 min (equilibration time); A from 20 to 40% in 10 min; A from 40 to 100% in 8 min; A 100% for 2 min, A from 100 to 20% in 2 min. For NA2: A 20% for 8 min (equilibration time); A from 20 to 60% in 10 min; A from 60 to 20% in 2 min. For NA3, NA4 and NA5 reaction products: A 20% for 8 min (equilibration time); A from 20 to 40% in 10 min; A from 40 to 20% in 2 min. The eluting products were detected at 230 nm, collected in Eppendorf tubes, dried at room temperature in Speed Vac UniVapo 100 H (UniEquip, Martinsried, Germany) and stored at 4°C if necessary. Analysis by liquid chromatography–mass spectrometry (LC–MS), direct infusion electrospray ionization (ESI) and tandem mass spectrometry were performed as previously described (7).

The reactivity of C was also evaluated using the following oligonucleotide, which contains only one cytosine within an AT-rich context: TAT ATT ATA ATT TAC AAA TAA ATT TAA AT (CL1-down, 8880.0 Da average molecular mass calculated from sequence). Sample mixtures were obtained by combining 10 μl of 10 mM CL in ethanol with 100 μl of 4.3 mM substrate in TE buffer (10 mM Tris, pH 7.4; 1 mM EDTA, pH 8.0), and incubating at 37°C for 24 h. The crude mixtures were analyzed by direct infusion ESI–MS in negative ion mode, as previously described (7).

NMR analysis

CL (5.4 mg, 3 mM) was incubated with ^{15}N-dC (5 mg, 4.2 mM, all three nitrogens were uniformly labeled) in H_2O:EtOH:TFA (50.95:30:0.05) at 37°C for 24 h. CL–^{15}N-dC adduct was separated and collected by HPLC as described above; the adduct solution was then dried in a lyophilizer (Heto, Denmark), yielding 2.4 mg of total product. CL–^{15}N-dC was dissolved in DMSO-d6 to give a final concentration of 7 mM.

All NMR spectra were acquired at 298 K on a Bruker Avance DRX 400 spectrometer (400.13 MHz proton frequency and 40.54 MHz ^{15}N frequency) equipped with a 5 mm multinuclear inverse *z*-field gradient probe-head. Data processing was performed on a Silicon Graphics O2 workstation using the XWIN-NMR software. ^{1}H and ^{15}N resonance assignments were obtained using 2D homonuclear correlation spectroscopy (DQF-COSY and NOESY) and 2D heteronuclear correlation spectroscopy (^{1}H–^{15}N HMQC and ^{1}H–^{15}N HMBC) with gradient coherence selection.

^{1}H monodimensional NMR spectra were acquired with eight transients, 4789 Hz spectral width, 32k data points. Double-quantum filtered correlation (DQF-COSY) (11) and nuclear Overhauser effect (NOESY) (12) experiments were recorded using a repetition delay of 1 s; a total of 512 experiments of 8 and 16 scans were accumulated; 2k data points were recorded in the acquisition dimension (F2) and the spectral width was 12 p.p.m. Zero-filling in both F1 and F2 multiplication with a gaussian function in F2 and a sine function (in DQF-COSY) or a squared cosine function (in NOESY) in F1 was performed prior to 2D Fourier transformation. In the NOESY experiment, the mixing period was 0.5 s. Assignment of the resonances in the ^{1}H NMR spectrum of the CL–^{15}N-dC adduct [chemical shifts in p.p.m. (italics), number of protons, multiplicity and position in the drug (CL) or nucleoside (dC) portion] were as follows: *0.8*, 3 H, s, CH_3-20CL; *0.95*, 3 H, d, CH_3-17CL; *1.13*, 3 H, s, CH_3-19CL; *1.24–2.40*, 14 H, m, CH_2-1CL, CH_2-2CL, CH_2-6CL, CH_2-7CL, CH-8CL, CH-10CL, CH_2-11CL, CH_2-2′dC; *3.60*, 2 H, ddd, CH_2-5′dC; *3.86*, 1 H, m, CH-4′dC; 4.05, 1 H, d, CH_2-12CL; *3.93* and *4.18*, 2 H, 2 d, CH_2-16CL; *4.23*, 1 H, m, CH-3′dC; *5.16*, 1 H, s, CH-15CL; *6.08*, 1 H, t, CH-1′dC; *6.35*, 1 H, m, CH-5dC; *6.69*, 1 H, t, CH-3CL; *8.29*, 1 H, d, CH-6dC; *9.25*, 1 H, s, CHO-18CL; *10.82*, 1 H, dd, NH-4dC.

The ^{1}H–^{15}N heteronuclear multiple-quantum correlation (HMQC) (13) spectrum was acquired using a repetition delay of 1 s; a total of 100 experiments of 128 scans were accumulated in the TPPI method (14), decoupling of ^{15}N with GARP sequence during acquisition, 5.6 ms evolution delay for $^1J_{HN}$ scalar coupling constants; the spectral width was 12 p.p.m. in F2, 300 p.p.m. in F1. Zero-filling in both F1 and F2 multiplication with a gaussian function (in F2) and a squared cosine function (in F1) was performed prior to 2D Fourier transformation. The ^{1}H–^{15}N heteronuclear multiple-bond correlation (HMBC) (15) spectrum was acquired using a repetition delay of 1 s; a total of 256 experiments of 512 scans were accumulated and processed with a magnitude calculation; 83 ms evolution delay was used for ^{1}H–^{15}N long-range coupling constants; the spectral width was 12 p.p.m. in F2, 400 p.p.m. in F1. Zero-filling in both F1 and F2 multiplication with a gaussian function (in F2) and a squared sine function (in F1) was performed prior to 2D Fourier transformation.

RESULTS

An intact C12–C15 ring is necessary for hot alkali-mediated DNA cleavage at single-stranded Cs

A systematic investigation using selected synthetic analogues was initiated to identify the structural features responsible for the attack/cleavage of cytidine by CL. For the sake of consistency with earlier work on the mechanism of reaction with G nucleotides, we initially utilized the same single-stranded substrate with sequence corresponding to one of the CL hot spots on SV40 (CL2640-up) (5–7). Based on previous findings that drug-induced cleavage at single-stranded C could be readily detected only after treatment with hot piperidine (6,7), this procedure was included in our standard assay of drug activity. Consequently, the level of C-alkylation was conveniently assessed by treating the substrate with variable concentrations of the different analogue drugs and by subsequently cleaving the products with hot piperidine.

The analogue NA1 with intact epoxide ring was immediately shown to induce efficient strand scission at all C sites present in the substrate sequence (i.e. positions 2644, 2643, 2631 of SV40, labelled as C2644, C2643, C2631 in Figure 2,

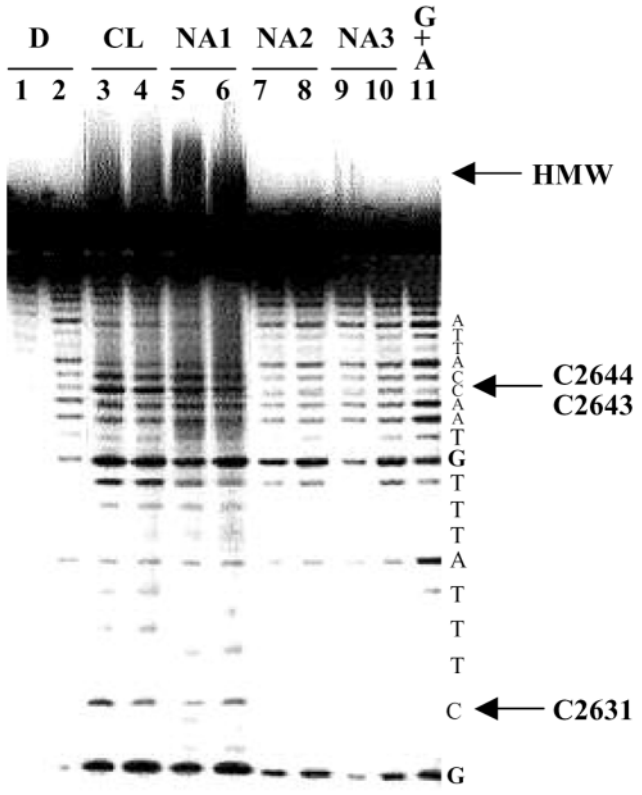

Figure 2. Reactivity of CL and NA derivatives toward single-stranded DNA. The oligonucleotide CL2640-up (see Materials and Methods) was 5′ end-labeled and reacted with 100 μM (odd lanes) or 200 μM (even lanes) concentrations of CL, NA1, NA2 and NA3. After treatment with 1 M piperidine at 90°C for 30 min, the products were analyzed by 20% denaturing acrylamide gels. Control lanes are shown as D: lane 1 contains non-treated oligo; lane 2 corresponds to oligo that was not exposed to any drug, but was directly submitted to hot alkali cleavage. Lane 11 contains a marker for purines (G + A) obtained by the Maxam and Gilbert reaction. Arrows mark the positions of susceptible cytosines (C2644, C2643 and C2631 refer, respectively, to positions 2644, 2643 and 2631 of the SV40 genome) and high molecular weight species (HMW). The susceptible guanines are marked in bold on the oligonucleotide sequence, which is reported on the right of the gel.

lanes 5 and 6), which is in excellent agreement with the results provided by the control reaction with the original CL structure (Figure 2, lanes 3 and 4). The product intensities were considerably higher than those of the control lane treated with piperidine (Figure 2, lane 2), but they were only slightly different between the CL and NA1 reactions (Figure 2, compare lanes 5 and 6 with 3 and 4), with the latter NA1 showing a higher activity at C2644 and C2643 and a lower activity at C2631. Further, both CL- and NA1-treated samples seemed to contain a number of higher molecular weight species (indicated as HMW in Figure 2, lanes 3–6), which migrated more slowly than the initial oligonucleotide itself. When NA2, NA3, NA4, NA5 were applied under similar conditions, no C-cleavage or HMW species were observed even at the highest drug concentration (Figure 2, data shown for NA2 and NA3 in lanes 7–10). It is important to note that while NA4 and NA5 proved to be similarly inert towards G, NA2 and NA3 were found instead to be fairly reactive towards this nucleotide (7) (see also Figure 2, lanes 7–10).

The drug analogues were also tested against a double-stranded structure to verify the previously observed preference of CL-induced scission for locally single-stranded structures of DNA (6). For this reason, a duplex construct was designed with a 3 nt bulge including an extruded C flanked by two Ts, in such a way as to combine an exposed target in the bulge with several protected Cs in the base-paired region of the same substrate (CL2640-up-C and CL2640-B-down). Samples were treated for increasing time intervals (0, 1, 6, 24 h) with different concentrations of CL and analogues. Also in this case, reaction mixtures were further treated with hot piperidine according to the Maxam and Gilbert protocol (10). Indeed, CL-control proved capable of inducing selective cleavage at the protruding C after alkali treatment, while the single-stranded flanking Ts were spared from specific damage. Base-paired nucleotides, including susceptible Cs and Gs, remained unreacted (Figure 3A). Mild cleavage at the bulging C was readily observed after 1 h reaction (Figure 3A, lanes 7 and 8) and increased considerably over time (Figure 3A, lanes 13, 14, and 19, 20). As expected, samples that were not treated with piperidine did not cleave as efficiently, but presented species with lower mobility, which appeared to be significantly reduced by the alkali treatment (Figure 3A, compare lanes 4, 5; 10, 11; 16, 17 with lanes 7, 8; 13, 14; 19, 20; respectively). It should be noted that the abundance of HMW species in samples with no piperidine treatment showed a striking correlation with the level of C bulge cleavage obtained by hot alkali reaction. Both features were barely detectable after 1 h incubation (Figure 3A, lanes 4, 5), but became increasingly evident after 6 and 24 h (Figure 3A, lanes 13, 14; 19, 20).

Under similar conditions, the NA analogues produced the results shown in Figure 3B. NA1 was found to induce cleavage at the bulging C with efficiency comparable to that of CL control (Figure 3B, compare lanes 7–10 with lanes 3–6), while NA2–NA5 analogues did not provide any detectable activity (Figure 3B, data shown for NA2 and NA3, lanes 11–18). HMW species were present in both NA1- and CL-treated samples and were reduced by hot piperidine, as described above (Figure 3B, compare lanes 7 and 8 with lanes 9 and 10 for NA1; lanes 3 and 4 with lanes 5 and 6 for CL). In contrast, no HMW products were observed upon incubation with NA2–NA5, providing further support to the importance of an intact epoxide for the reactivity to C nucleotides.

Epoxide and C14-carbonyl are both necessary for C-reactivity

The prominent formation of HMV species, which are detected as well-resolved bands with lower electrophoretic mobility, and their prompt elimination upon application of the Maxam and Gilbert reagents provide strong indications that the mechanism of action of CL involves the formation of a covalent adduct with exposed C nucleobases in single-stranded positions. This hypothesis was tested by investigating the reaction of CL and analogues with isolated 2′-deoxy-cytosine (dC), using reverse-phase HPLC and HPLC–MS to monitor the adduct formation at different time intervals.

Adducts were first identified by differential analysis of HPLC chromatograms. The ratio between the area of the

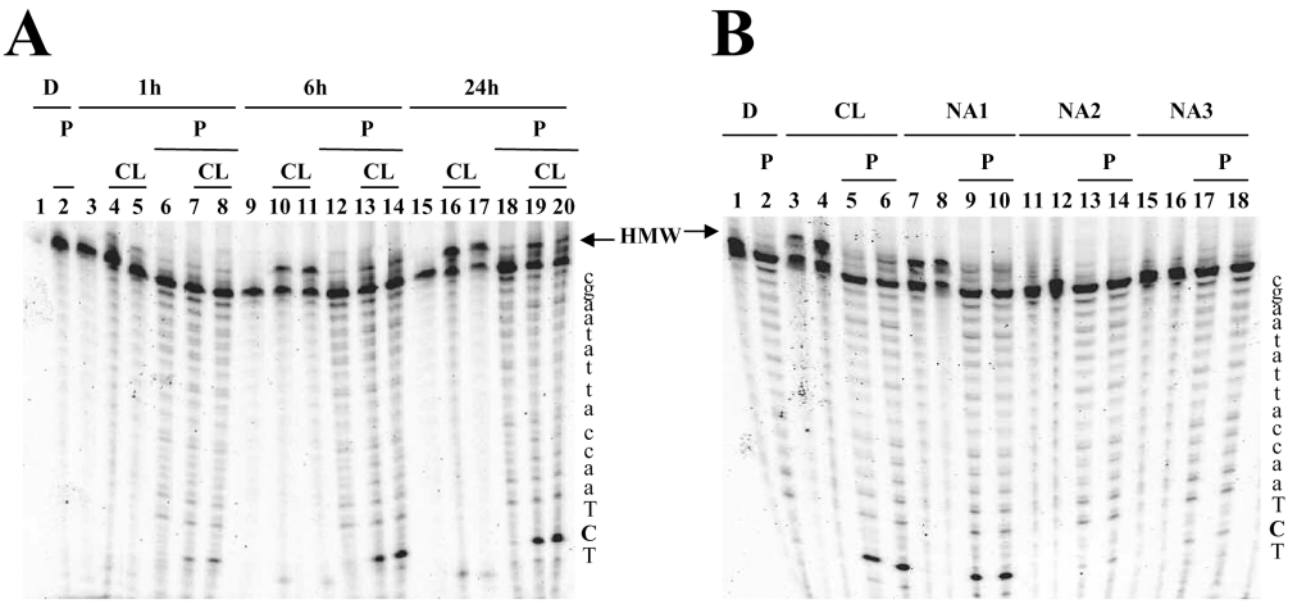

Figure 3. Reactivity of CL and NA derivatives toward C-bulged DNA. (**A**) The stable duplex with TCT bulge (see Materials and Methods) was reacted with 100 μM (lanes 4, 7, 10, 13, 16, 19) and 200 μM (lanes 5, 8, 11, 14, 17, 20) of CL for the indicated times. Aliquots were further treated with 1 M piperidine at 90°C for 30 min and all samples were loaded onto 20% denaturing acrylamide gels. Only products provided by the labeled strand CL2640-up-C are detectable. Control lanes are shown as D: lane 1 contains non-treated oligo; lane 2 corresponds to oligo that was not exposed to the drug, but was directly submitted to hot alkali cleavage. P indicates piperidine-treated samples. (**B**) The same duplex substrate was reacted with 100 μM (odd lanes) and 200 μM (even lanes) concentrations of NA1, NA2 and NA3. Also in this case, only products provided by the labeled strand CL2640-up-C are detectable. Control lanes are shown as D: lane 1 contains non-treated oligo; lane 2 corresponds to oligo that was not exposed to any drug, but was directly submitted to hot alkali cleavage. P indicates piperidine-treated samples. The oligonucleotide resolved sequence is reported on the right of each the gel; the bulged nucleotides are shown in upper case, the cleaved C in bold. High molecular weight species (HMW) are marked by arrows.

adduct peak and the total area of peaks detected in each chromatogram was calculated to obtain the reaction yields. In this way, CL and NA1 were found to provide comparable yields (75.0% and 73.8%, respectively, after 48 h at 37°C), while NA2 produced a negligible yield (1.1%) under the same conditions (Figure 4A). No adducts could be detected for NA3–NA5, which remained completely inactive even after extended incubation at significantly higher temperature (i.e., 60°C). The chromatographic fractions corresponding to dC adducts with CL and NA1 were collected and analyzed by electrospray ionization coupled with a time-of-flight mass analyzer (ESI–TOF-MS). Molecular masses obtained for these species matched 1:1 covalent adducts of 2′-deoxy-cytosine with the drugs (576.2 Da for CL, shown in Figure 4B; 498.1 Da for NA1, not shown).

An oligonucleotide containing a single C in an AT context (CL1-down) was employed to confirm the ability of CL and analogues to form stable covalent adducts when C is present in a single-stranded structure. Reactions were performed as described in the Materials and Methods section and the product mixtures were analyzed directly by ESI after 24 h incubation at 37°C. The formation of CL monoadduct was immediately observed with a characteristic incremental mass (Δ = 348.2 Da, Figure 4C), which confirmed the ability of CL to alkylate C, but not T and A. Further, no cleavage products could be detected, thus proving that alkylation cannot induce strand cleavage *per se* under the selected experimental conditions. Finally, no adducts could be observed for NA2 and NA3, consistent with the required presence of C14 electrophiles and an intact vicinal epoxide for covalent reaction to C.

Structure of CL–dC adduct

Tandem mass spectrometry. The possible structure of the CL–dC adduct should not only be consistent with the observed reactivity pattern, but should also account for the fact that both the epoxide and C14 of CL are involved in the nucleophilic attack and that the cytidine structure presents at least three nucleophilic groups, which could be targeted by the drug electrophilic functions: the exocyclic amino group (NH_2), the pyrimidine nitrogen N3, and the oxygen in position 2 (O2).

Direct structural characterization of the CL–dC adduct was performed by tandem mass spectrometry (16). The fragmentation pattern obtained by gas-phase activation of a selected precursor ion is diagnostic of the precursor structure and can be effectively employed to characterize nucleic acid adducts (17,18). Dissociation experiments were performed off-line on isolated HPLC fractions using a Fourier transform mass spectrometer (FTMS) (19,20). Abundant product ions were detected in positive ion mode upon activation of protonated CL–dC adduct, which are consistent with the putative structures provided in Figure 5B. The observed fragmentation pattern is indicative of a cyclic structure in which the exocyclic amino group (NH_2) of dC is bound to C14 of CL, whereas N3 has reacted with the epoxide to form a condensed ring system. The observed cleavage of the N-glycosidic bond with loss of the sugar moiety (*m/z* 460.2) is a typical gas-phase process facilitated by alkylation of the pyrimidine ring. Loss of three molecules of water and CO are consistent with the presence of alcoholic functions and aldehydic groups. Due to the relatively higher gas-phase basicity of the cytosine moiety, the

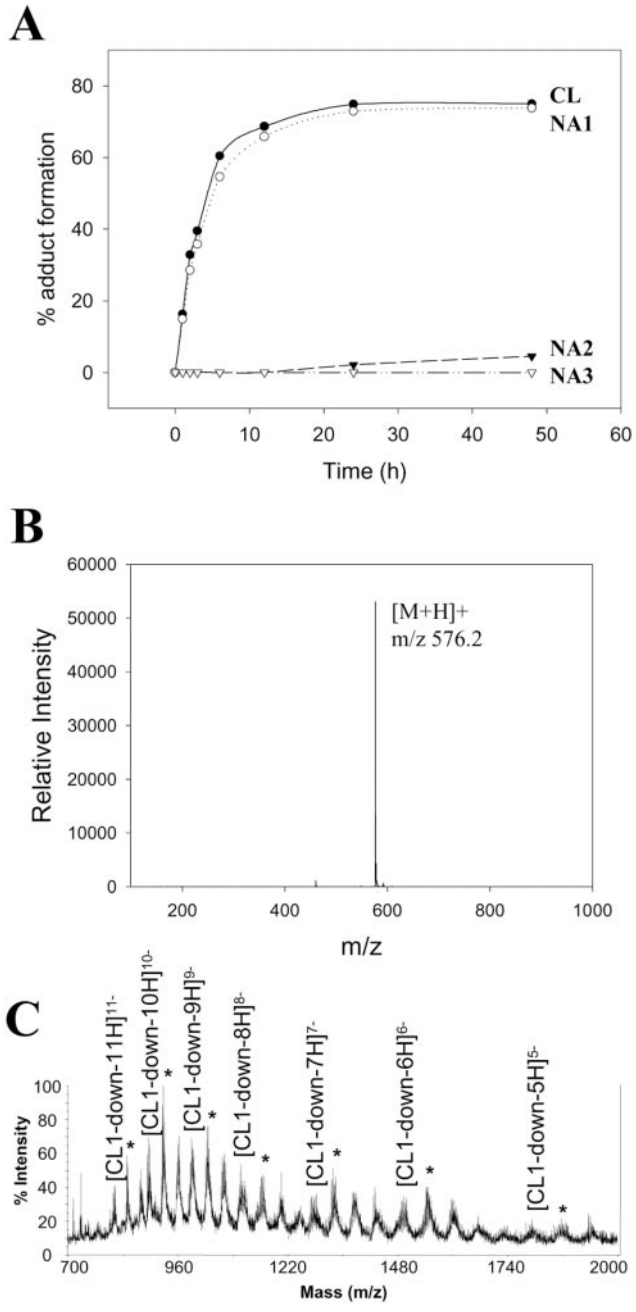

Figure 4. HPLC and ESI–MS analysis of drug adducts. (**A**) Time-course of the reactions of CL and analogues with dC. The incubation temperature was 37°C for reaction with CL, NA1 and NA2, while 60°C was used for NA3. Reaction mixtures were sampled at 1, 2, 3, 6, 12, 24, 48 h and analyzed by reversed-phase HPLC with detection at 230 nm. For each drug, the percentage of adduct formation was calculated from the ratio of the area of the respective chromatographic peak over the total peak area. (**B**) ESI–MS spectrum of CL–dC adduct. The chromatographic peak corresponding to the CL–dC adduct was collected and analyzed by direct infusion ESI–MS in positive ion mode to determine its molecular mass. The observed value of 576.2 Da is in good agreement with the monoisotopic mass calculated for the protonated ion of a 1:1 CL–dC adduct (576.3 Da). (**C**) ESI–MS spectrum of CL reaction with CL1-down, a single-stranded AT oligonucleotide including a single C. The oligonucleotide was detected in negative ion mode as a polyanionic species with charge states ranging from −11 to −5 (indicated as $[CL1\text{-down} - nH]^{n-}$). The observed average molecular mass of 8881.5 ± 20.6 Da is in excellent agreement with the mass calculated from sequence (8880.0 Da average molecular mass). Signals corresponding to the CL mono-adduct are marked by an asterisk and present the characteristic mass shift of 348.2 Da.

diterpenoid portion is lost as neutral and is not detected, while the positive charge is retained by the remaining fragment. The latter includes the two-condensed ring system (*m/z* 194.0, 168.0) proposed for the adduct structure, which appears to be particularly stable in the gas-phase. In conclusion, these fragments suggest a putative structure produced by two nucleophilic attacks, including one performed by the cytidine primary amino group towards the C14 carbonyl of CL, and the other by N3 to the strained epoxide ring to complete a stable condensed system (Figure 5A).

NMR analysis. Further structural characterization was obtained by NMR analysis of the isolated drug–nucleoside adduct. In this case, the necessary amount of analyte was obtained by scaling up the reaction and by employing ^{15}N-enriched dC as a substrate. The reaction reached completion after 24 h at 37°C, when almost all the initial drug was converted into CL–^{15}N-dC adduct. The labeled sample was subsequently purified by HPLC as described for the small-scale, unlabeled sample.

The ^{1}H NMR spectrum of CL–^{15}N-dC is shown in Figure 6A and the proton resonance assignments are included in Materials and Methods. In comparison with an analogous ^{1}H spectrum obtained for a freshly dissolved solution of CL (5), we observed downfield chemical shifts for CH_2-16 and CHO-15, and an upfield shift for CH_2-12 of the CL portion, which confirm that the C12–C15 ring system is primarily involved in the reaction with the nucleoside. Downfield chemical shifts were detected only for the pyrimidine moiety (CH-5 and CH-6), while the ribose resonances resulted essentially unchanged from the H^1 spectrum of unreacted ^{15}N-dC (data not shown). Further, the signal for the amino protons in N4 shifted from 7.08 to 10.82 p.p.m. for the reacted sample and integrated for only one proton, instead of two, strongly suggesting the presence of an extra bond at this site.

The assignment of the resonances in the ^{1}H NMR spectrum was confirmed by the analyses of the DQF-COSY and the NOESY spectra (data not shown). The functionalities responsible for CL–dC adduct formation were further investigated by performing bidimensional ^{1}H–^{15}N heteronuclear correlation spectroscopy. The ^{1}H–^{15}N HMBC spectrum in Figure 6B, which offers peaks arising from long-range scalar coupling, shows two signals that are diagnostic of the adduct structure. In fact, the two protons at position 16 of CL were found to couple with N3 of dC (140.4 p.p.m.), indicating that the epoxide had reacted at the N3 position of the base. The proton in position 15 shows coupling with N4 of dC (129.2 p.p.m.), thus confirming the presence of a covalent bond between C14 of the drug and N4 of the nucleoside. Other proton signals from the ribose moiety are in perfect agreement with the expected data: positions 1′ and 2′ were coupled with N1 (157.7 p.p.m.); positions 5 and 6 were coupled with all three nitrogens; the amine proton at N4 was coupled to N3, and through one-bond coupling constant to N4. The assignment of the N4 resonance was confirmed by the HMQC spectrum, where just one-bond scalar couplings are evident (Figure 6C). In conclusions, these NMR data are in excellent agreement with those provided by tandem mass spectrometry and confirm unequivocally the proposed adduct structure (Figure 5A).

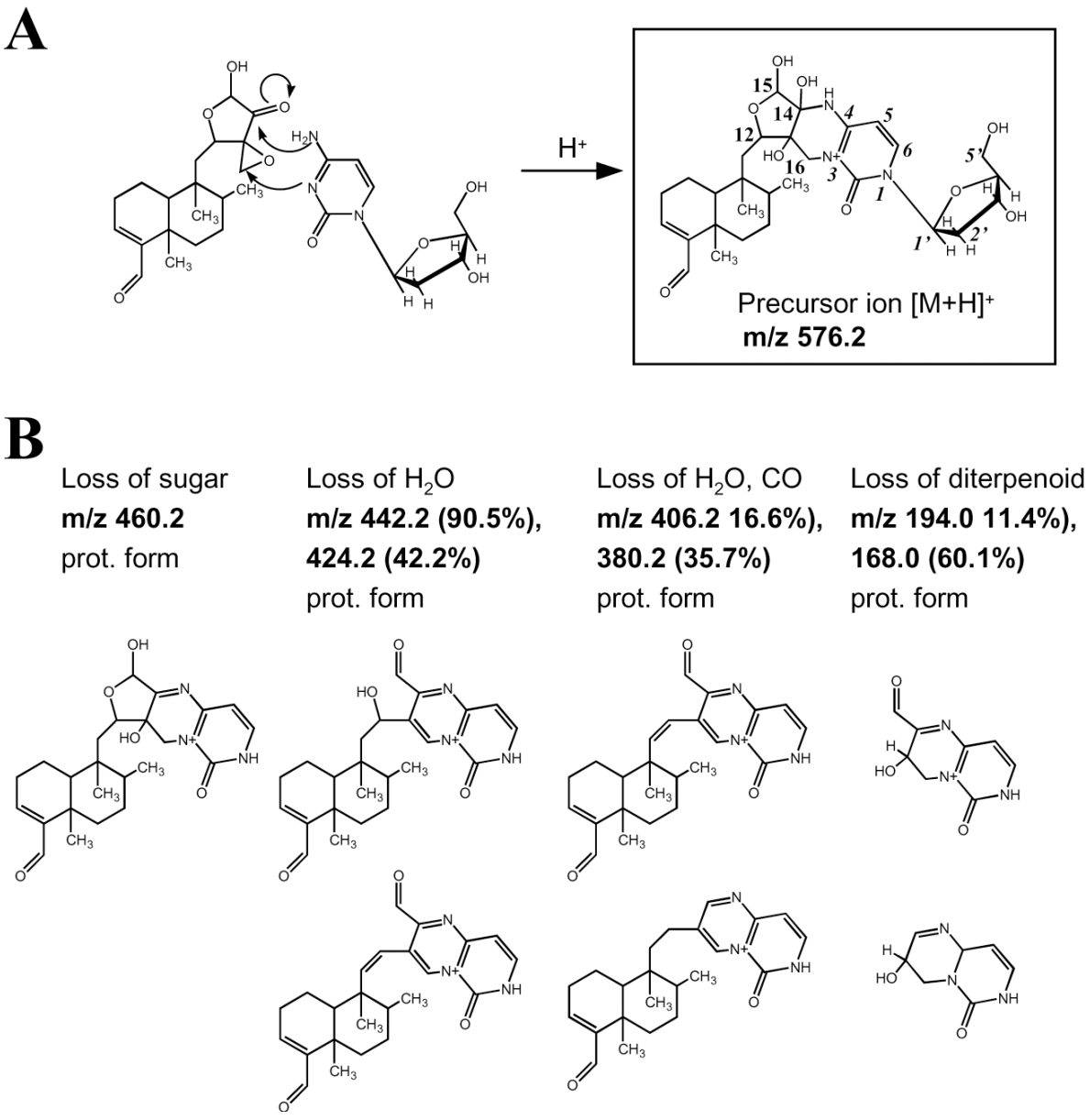

Figure 5. CL–dC adduct structure. (**A**) Reaction scheme of CL with dC. The nucleophilic amino group of the pyrimidine ring attacks the electron acceptor C14 atom of the carbonyl function. Activated by the vicinal carbonyl moieties and by the spiro ring system, the epoxide function is put within striking distance from the nucleophilic N3 of cytosine and performs an electrophilic attack. The addition of one proton neutralizes the negative charge of the oxygen of the open epoxide. A positively charged species is formed, which is stable and can be readily detected by ESI–MS analysis. Numeration is provided for the boxed CL–dC structure. Bold numbers refers to CL atoms, italicized numbers mark the nucleobase portion, and apex symbols are used for the sugar moiety of dC. (**B**) Interpretation of fragment ions obtained by tandem mass spectrometry of protonated CL–dC adduct (*m/z* 576.2). The relative intensity of each fragment ion is indicated between parentheses.

Kinetics of CL–dC versus CL–dG adduct

Double-stranded structures containing a locally single-stranded C or G were utilized to compare the kinetics of CL–dC and CL–dG formation in a more structured environment. In particular, we utilized two duplex constructs with identical sequence, save for the presence of either a TCT or a TGT bulge [see Materials and Methods and (6)]. Samples were treated with selected concentrations of CL for different time intervals (0, 1, 6, 24 h) and then added with hot piperidine (10). Such a treatment was found to induce selective cleavage at the target G and C sites (see lanes 5–10 for G and 15–20 for C, Figure 7A). In particular, CL was proved to induce mild C-cleavage after 1 h at the higher concentration (lane 18, Figure 7A), while strand breaks increased significantly over time at either concentration (lanes 16, 17 and 19, 20, Figure 7A). These samples contained also species with lower mobility (HMW), which were not completely eliminated by treatment with hot alkali. On the contrary, no strand breaks were detected at G after 1 h (compare lanes 5 and 8 with control lanes 1–4, Figure 7A), but became apparent only after more extensive incubation (6–24 h, lanes 6, 9 and 7, 10, Figure 7A). No HMW species were observed in this case. A quantitative examination of CL effects at either the C or the G bulge

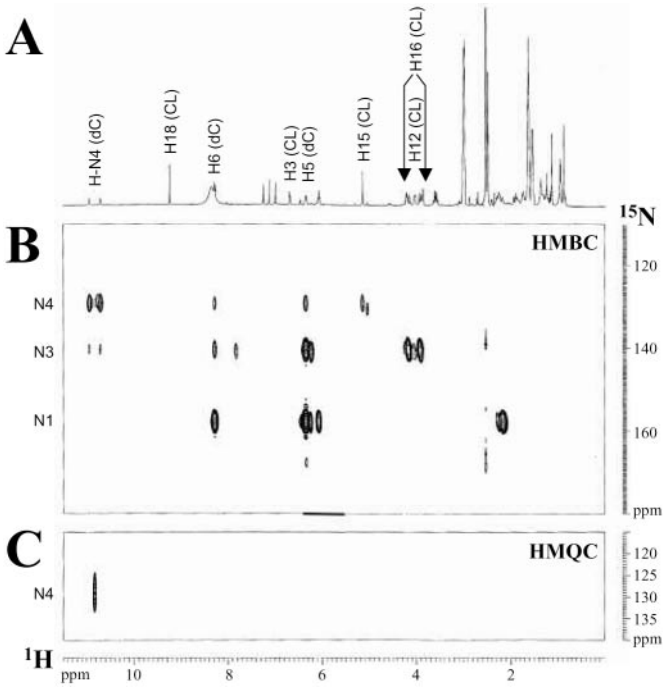

Figure 6. NMR analysis: (**A**) ^{1}H monodimensional NMR spectra of CL–^{15}NdC adduct; (**B**) ^{1}H–^{15}N HMBC and (**C**) ^{1}H–^{15}N HMQC spectra of CL–^{15}NdC adduct.

(Figure 7B) suggests that the reaction with C is at least three times faster than with G in a DNA environment. This is consistent with the observation that isolated dC is also attacked more rapidly than dG in solution (data not shown).

Following CL reaction, the duplex with TCT bulge was subjected to hot piperidine treatment for increasing time intervals to test whether the HMW products could be completely eliminated by boosting the strand scission at the bulged C. As suspected, HMW species were found to be gradually degraded by hot alkali with a concomitant increase of the products of C-cleavage (Figure 7C, lanes 2–6). These results strongly support the hypothesis that HMW may correspond to a stable CL-adduct at the bulged C, which can only undergo base elimination upon harsh alkali treatment.

DISCUSSION

The mechanism of action of CL as a topoisomerase II poison is made intriguing by its ability to induce strand breaks at G and C *per se* (6) and form both reversible and irreversible ternary complexes with the eukaryotic enzyme and DNA (5). We have shown that G-damage is induced by N7-alkylation, followed by spontaneous depurination and strand scission (7), while cleavage at C can only be observed upon treatment with hot alkali. This reactivity profile is limited to Cs present in single-stranded regions or located in locally distorted nucleic acid structures, as indicated by the results provided by the bulged duplex. In this respect, molecular modeling simulations have clearly demonstrated that CL fits poorly in either grooves of double-helical DNA (6). Consequently, CL may be able to reach its targets only when the conformation of the nucleic acid substrate is substantially distorted.

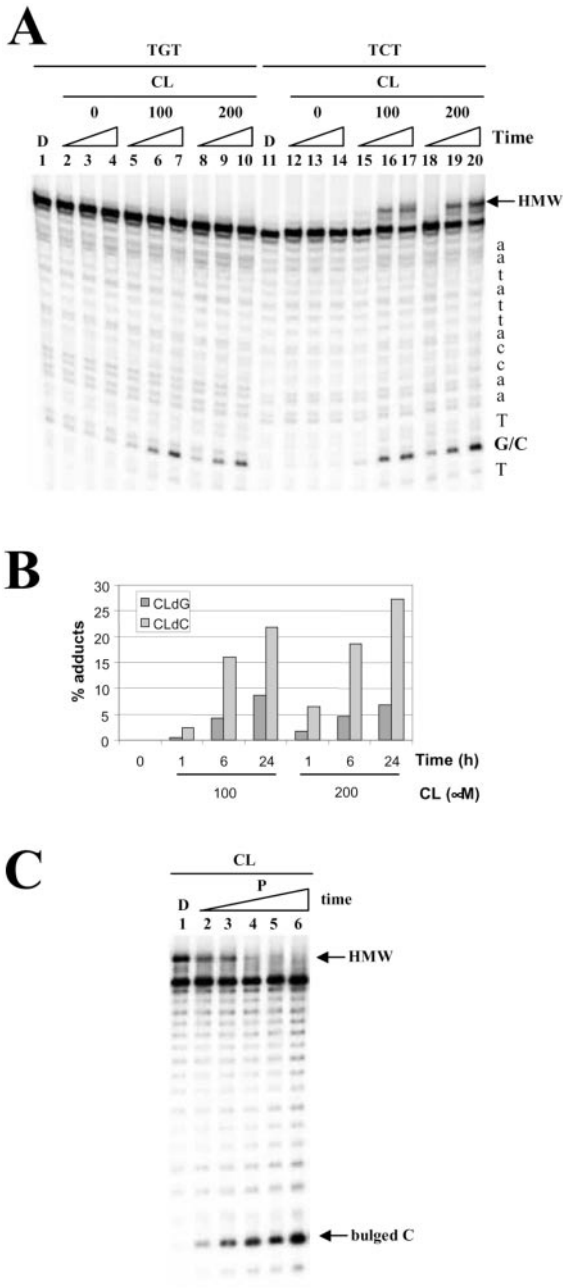

Figure 7. Kinetics of CL reactivity. (**A**) Reactivity toward C- and G-bulged DNA. The bulged oligonucleotides were reacted with CL at 100 (lanes 5, 6, 7 and 15, 16, 17) or 200 (lanes 8, 9, 10 and 18, 19, 20) μM for 1 h (lanes 2, 5, 8, 12, 15, 18), 6 h (lanes 3, 6, 9, 13, 16, 19) and 24 h (lanes 4, 7, 10, 14, 17, 20). All samples were further treated with 1 M piperidine at 90°C for 30 min and loaded on 20% denaturing acrylamide gels. Control lanes are shown as D: lane 1 is the non-treated oligo; lanes 2–4 and 12–14 contain non-reacted oligo treated in the same conditions as samples reacted with the drugs. Sample identities are indicated above the gel (bulge TGT or TCT). The resolved sequence is reported on the right of the gel; bulged nucleotides are shown in upper case; cleaved C or G are in bold; high molecular weight species (HMW) are marked by arrows. (**B**) Quantification of CL effects on bulged C and G DNA. Quantification of samples 4–10 and 14–20 of panel B are plotted. Adducts are comprehensive of HMW and cleavage bands. (**C**) Kinetics of piperidine treatment. The TCT-bulged oligonucleotide was reacted with 200 μM CL for 24 h. After DNA precipitation, samples 2–6 were resuspended in 1 M piperidine and incubated at 90°C for 0.4, 0.2, 1, 2, 3 h, respectively (P stands for piperidine). D is a control lane for the oligo treated with CL, with no piperidine incubation. HMW species and the site of C cleavage are shown on the right.

The fact that different mechanisms are followed to achieve strand scission is not the only indication that CL presents two clearly distinct modes of interaction with cytidine and guanine. This distinction is also evident from the roles played by the different functional groups of CL when either substrate is involved. An intact C12–C15 ring system is necessary to induce C-alkylation, while reduction of the C14 carbonyl function (NA2 and NA3) and opening of the oxirane group (NA4 and NA5) result in complete drug inactivation. On the contrary, an intact epoxide constitutes the sole requirement for G-alkylation, while the carbonyls act as modulators of oxirane reactivity through preservation of the *spiro* system (7). In each case, the diterpenoid moiety appears to be dispensable, as demonstrated by the conserved reactivity of the naphthalene analogue (NA1) towards both substrates.

The structural information obtained by tandem mass spectrometry and NMR confirmed the formation of a product resulting from the concerted nucleophilic attack of NH_2 and N3 of dC towards the adjacent C14 and C16 of CL, respectively. This double alkylation allows for the formation of a stable condensed ring system (Figure 5A), which can further undergo closure to the stabilized hemi-acetalic form of the C12–C15 portion of CL. In principle, a reaction could also occur between NH_2 and the aldehyde at C15, but the amount of covalent adduct observed for NA2 was negligible even after long incubation, thus making this route less favorable.

This interpretation is consistent with the results of theoretical calculations based on molecular models, which suggest that the epoxide and C14 are the most electrophilic centers in the CL structure (S. Moro, personal communication), and with earlier experiments showing that both epoxide and C14-carbonyl may yield adducts, the former through nucleophilic attack and opening of the oxirane ring, the latter through formation of a Shiff-base with the substrate amino group (9). From the cytosine point of view, alkylation of O2 is known to undermine the stability of the adjacent N-glycosidic bond, which can readily undergo spontaneous cleavage in solution (21). In our case, however, no hydrolysis was detected and the adduct proved to be very stable. On the other hand, N3 is known for being effectively attacked by many alkylating agents, among which dimethylsulfate and methylnitrosourea (22,23) and has emerged as the most nucleophilic center in a recent computational study that compared the activation energies in aqueous environment for the alkylation of the three nucleophilic sites of C (24). For these reasons, two subsequent nucleophilic reactions could be envisaged, including the fast initial formation of an α-hydroxy amine between the primary amino group of C and the C14-carbonyl, which is followed by intramolecular reaction of the epoxide with N3 of the pyrimidine ring. This sequence of events could also explain the different reaction rates observed for C and G, considering that the rate-determining intramolecular attack of cytosine N3 to the epoxide is characterized by an increased frequency of collision between electrophilic and nucleophilic centers, whereas this is not the case for the intermolecular alkylation involving guanosine N7.

The proposed CL–dC structure can be invoked to explain the only partial degradation induced by piperidine treatment under standard DNA sequencing conditions (1 M piperidine at 90°C for 30 min) (10,25,26). In fact, dimethylsulfate, hydrazine and similar chemicals used in DNA sequencing are known to attack susceptible bases and induce electron rearrangements, which can cause ring opening and/or destabilization of the N-glycosidic bond. In a similar way, CL reaction introduces a positive charge into the guanine moiety, which becomes a good leaving group for alkali-induced base elimination. This effect does not materialize for cytosine, in which a second alkylation process induces a prompt intramolecular closing of the adduct structure, thus compensating for any destabilization introduced by the initial CL reaction. As a result, this adduct is relatively stable to hot piperidine treatment, which requires longer than the standard 30 min to fully convert all HMW species during strand scissions at the bulged C.

The possible formation of additional intramolecular hydrogen bonds between adjacent hydroxyl groups on C13, C14 and C15 is likely to introduce further stabilization into the product and may explain, for example, the lack of dehydration of the α-hydroxy amine observed after closing of the adduct structure. This observation is consistent with the fact that aqueous environments favor the formation of hydrated species in solution, which tend to readily lose water molecules upon gas-phase activation during tandem mass spectrometry.

Finally, comparing the structures of the guanine and cytosine adducts offers important clues on the possible mechanism of drug-stimulated DNA cleavage in the presence of topoisomerase II, which was completely irreversible when G was located at the 3′ end of the cleaved site, but was found to be reversible when C was present (5). Although the latter observation seems to clash with the very stable and irreversible nature of this covalent adducts, its meaning becomes immediately clear when considering that, upon cleavage by topoisomerase II, the bases at position −1 could still remain paired with their complementary counterparts to allow for prompt re-ligation (27). In this case, the NH_2 and N3 positions of cytosine, which are involved in base-pairing, would be effectively protected from CL alkylation, thus rendering the cleavage complex reversible. On the contrary, the N7 of guanine is not involved in base pairing and would still be exposed to efficient alkylation, which would make re-ligation impossible and DNA damage irreversible.

In conclusion, CL may be depicted as a multi-functional drug, whose preferred mechanism may be different according to time and enzyme activity. For relatively long reaction times, CL can induce spontaneous depurination at G and produce stable covalent adducts with exposed C, which only become apparent *in vitro* upon alkali treatment. In the presence of topoisomerase II and in a time scale sufficient for enzymatic reaction, CL can still form covalent adducts with G at −1 of cleaved sites, while the lack of alkylation at a protected −1 cytosine explains the reversible nature of the damage at these sites and manifest CL as a classic (reversible) topoisomerase II poison. The comprehension of the mode of action of CL towards the DNA both in the presence and absence of topoisomerase II is a first essential step to the potential development of new more specific antitumor drugs with novel and modulated mechanism of action.

ACKNOWLEDGEMENTS

This work was supported by Associazione Italiana Ricerche sul Cancro (AIRC) and Ministero Istruzione, Università e Ricerca (MIUR).

REFERENCES

1. Andersen,N.R., Lorck,H.O. and Rasmussen,P.R. (1983) Fermentation, isolation and characterization of antibiotic PR-1350. *J. Antibiot. (Tokyo)*, **36**, 753–760.
2. Kawada,S., Yamashita,Y., Ochiai,K., Ando,K., Iwasaki,T., Takiguchi,T. and Nakano,H. (1995) Terpentecin and UCT4B, new family of topoisomerase II targeting antitumor antibiotics produced by *Streptomyces*: producing organism, fermentation and large scale purification. *J. Antibiot. (Tokyo)*, **48**, 211–216.
3. McCullough,J.E., Muller,M.T., Howells,A.J., Maxwell,A., J,O.S., Summerill,R.S., Parker,W.L., Wells,J.S., Bonner,D.P. and Fernandes,P.B. (1993) Clerocidin, a terpenoid antibiotic, inhibits bacterial DNA gyrase. *J. Antibiot. (Tokyo)*, **46**, 526–530.
4. Kawada,S., Yamashita,Y., Fujii,N. and Nakano,H. (1991) Induction of a heat-stable topoisomerase II-DNA cleavable complex by nonintercalative terpenoides, terpentecin and clerocidin. *Cancer Res.*, **51**, 2922–2925.
5. Binaschi,M., Zagotto,G., Palumbo,M., Zunino,F., Farinosi,R. and Capranico,G. (1997) Irreversible and reversible topoisomerase II DNA cleavage stimulated by clerocidin: sequence specificity and structural drug determinants. *Cancer Res.*, **57**, 1710–1716.
6. Gatto,B., Richter,S., Moro,S., Capranico,G. and Palumbo,M. (2001) The topoisomerase II poison clerocidin alkylates non-paired guanines of DNA: implications for irreversible stimulation of DNA cleavage. *Nucleic Acids Res.*, **29**, 4224–4230.
7. Richter,S., Gatto,B., Fabris,D., Takao,K., Kobayashi,S. and Palumbo,M. (2003) Clerocidin alkylates DNA through its epoxide function: evidence for a fine tuned mechanism of action. *Nucleic Acids Res.*, **31**, 5149–5156.
8. Kawada,S.Z., Yamashita,Y., Uosaki,Y., Gomi,K., Iwasaki,T., Takiguchi,T. and Nakano,H. (1992) UCT4B, a new antitumor antibiotic with topoisomerase II mediated DNA cleavage activity, from *Streptomyces* sp. *J. Antibiot. (Tokyo)*, **45**, 1182–1184.
9. Richter,S., Fabris,D., Binaschi,M., Gatto,B., Capranico,G. and Palumbo,M. (2004) Effects of common buffer systems on drug activity: the case of Clerocidin. *Chem. Res. Toxicol.*, **17**, 492–501.
10. Maxam,A.M. and Gilbert,W. (1980) Sequencing end-labeled DNA with base-specific chemical cleavages. *Meth. Enzymol.*, **65**, 499–560.
11. Ancian,B., Bourgeois,I., Dauphin,J.F. and Shaw,A. (1997) Artifact-free pure absorption PFG-enhanced DQF-COSY spectra including a gradient pulse in the evolution period. *J. Magn. Reson. A*, **125**, 348–354.
12. Wagner,R. and Berger,S. (1996) Gradient-selected NOESY—a fourfold reduction of the measurement time for the NOESY experiment. *J. Magn. Reson. A*, **123**, 119–121.
13. Bax,A., Griffey,R. and Hawkins,B.L. (1983) Correlation of proton and nitrogen-15 chemical shifts by multiple quantum NMR. *J. Magn. Reson. A*, **55**, 301.
14. Marion,D. and Wuthrich,K. (1983) Application of phase sensitive two-dimensional correlated spectroscopy (COSY) for measurements of 1H–1H spin–spin coupling constants in proteins. *Biochem. Biophys. Res. Commun.*, **113**, 967–974.
15. Bax,A. and Summers,M.F. (1986) Proton and carbon-13 assignments from sensitivity-enhanced detection of heteronuclear multiple-bond connectivity by 2D multiple quantum NMR. *J. Am. Chem. Soc.*, **108**, 2093–2094.
16. McLafferty,F.W. (1981) Tandem mass spectrometry. *Science*, **214**, 280–287.
17. Beck,J.L., Colgrave,M.L., Ralph,S.F. and Sheil,M.M. (2001) Electrospray ionization mass spectrometry of oligonucleotide complexes with drugs, metals, and proteins. *Mass Spectrom. Rev.*, **20**, 61–87.
18. Zhang,Q., Ding,Z., Creighton,D.J., Ganem,B. and Fabris,D. (2002) Alkylation of nucleic acids by the antitumor agent COMC. *Org. Lett.*, **4**, 1459–1462.
19. Comisarow,M.B. and Marshall,A.G. (1974) Fourier transform ion cyclotron resonance. *Chem. Phys. Lett.*, **25**, 282–283.
20. Marshall,A.G., Hendrickson,C.L. and Jackson,G.S. (1998) Fourier transform ion cyclotron resonance mass spectrometry: a primer. *Mass Spectrom. Rev.*, **17**, 1–35.
21. Singer,B., Kroger,M. and Carrano,M. (1978) O2- and O4-alkyl pyrimidine nucleosides: stability of the glycosyl bond and of the alkyl group as a function of pH. *Biochemistry*, **17**, 1246–1250.
22. Singer,B. and Grunberger,D. (1983) *Molecular Biology of Mutagens and Carcinogens*. Plenum Press, New York.
23. Rokita,S.E., Yang,J., Pande,P. and Greenberg,W.A. (1997) Quinone methide alkylation of deoxycytidine. *J. Org. Chem.*, **62**, 3010–3012.
24. Freccero,M., Di Valentin,C. and Sarzi-Amade,M. (2003) Modeling H-bonding and solvent effects in the alkylation of pyrimidine bases by a prototype quinone methide: a DFT study. *J. Am. Chem. Soc.*, **125**, 3544–3553.
25. Donis-Keller,H., Maxam,A.M. and Gilbert,W. (1977) Mapping adenines, guanines, and pyrimidines in RNA. *Nucleic Acids Res.*, **4**, 2527–2538.
26. Maxam,A.M. and Gilbert,W. (1977) A new method for sequencing DNA. *Proc. Natl Acad. Sci. USA*,**74**, 560–564.
27. Hiasa,H., Yousef,D.O. and Marians,K.J. (1996) DNA strand cleavage is required for replication fork arrest by a frozen topoisomerase-quinolone-DNA ternary complex. *J. Biol. Chem.*, **271**, 26424–26429.